

Gas Permeation in Miscible Blends of Poly(methyl methacrylate) with Bisphenol Chloral Polycarbonate

J. S. CHIOU and D. R. PAUL, *Department of Chemical Engineering and Center for Polymer Research, University of Texas, Austin, Texas 78712*

Synopsis

The miscibility of poly(methyl methacrylate) (PMMA) with bisphenol chloral polycarbonate (BCPC) has been studied using differential scanning calorimetry (DSC), optical indication of phase separation on heating (i.e., lower critical solution temperature (LCST) behavior), density measurement, and gas permeation. All evidence indicates that PMMA is miscible with BCPC over the whole blend composition range. Single composition-dependent glass transition temperature and LCST behavior have been observed for each blend. The specific volumes of the blends follow closely the simple additivity rule indicating the interaction between PMMA and BCPC is weak. Gas permeability coefficients for He, H₂, O₂, Ar, N₂, CH₄, and CO₂ measured at 35°C under 1 to 2 atm upstream pressure are lower than those calculated from the semilogarithmic additivity rule. The difference between this calculated permeability and the measured one increases with gas molecular size. As a result, the ideal gas separation factors for He/CH₄, CO₂/CH₄, and O₂/N₂ gas pairs estimated from the ratio of pure gas permeabilities are higher than predicted from the semilogarithmic additivity rule. These permeation results were interpreted in terms of the free volume theory and the activated state theory, which have been proposed to describe gas transport behavior in polymer mixtures.

INTRODUCTION

Previous studies have shown that information about the state of mixing of blends can be learned from the dependence of gas permeability on blend composition.¹ The gas permeability coefficient, P , when plotted semilogarithmically versus the blend composition in terms of volume fraction, ϕ , often shows a linear relationship when the blends are miscible (1–4), i.e.,

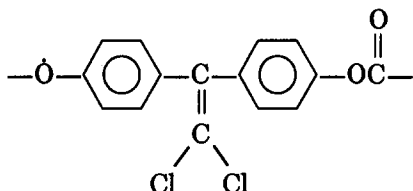
$$\ln P = \phi_1 \ln P_1 + \phi_2 \ln P_2 \quad (1)$$

On the other hand, an S-shape relationship between $\ln P$ and ϕ is usually observed for blend systems which are immiscible.^{5–12} This contrast allows one to distinguish a miscible blend system from an immiscible one.

The rationale for the simple mixing rule shown in Eq. (1) for miscible blends stems from both free volume theory and activated state theory as shown recently by Paul.¹³ Indeed, it is a special case of more general equations as explained later. Moreover, the deviations from this simple rule have been found to increase with the gas molecular size when the two component polymers in the blend have strong interactions.^{14–16} This finding has an important bearing on the application of polymer blends to gas separations by

membranes since separation factors for blends can be higher than predicted from the semilogarithmic rule and, in some cases, can be even higher than those of the component polymers.^{14,15} However, relevant studies on this subject are limited.

To extend our knowledge in this area we have investigated gas transport behavior in several miscible blend systems.^{4,14-19} This paper reports results for blends of poly(methyl methacrylate) (PMMA), and bisphenol chloral polycarbonate (BCPC). The latter has the following repeat unit



and is a highly flame-resistant polymer.²⁰ It has mechanical properties close to bisphenol-A polycarbonate, (PC) and has been reported to be miscible with PC.²⁰ Recent miscibility studies in our laboratory have shown that PMMA is miscible with both BCPC and PC, although earlier reports state that PMMA is immiscible or partially miscible with PC.²¹⁻²⁵ A re-examination of the miscibility of PMMA/PC blends has been described elsewhere.²⁶ In this communication, the miscibility of PMMA/BCPC blends will be discussed first followed by investigation of the gas transport properties of the blends.

EXPERIMENTAL

The PMMA used in this study was a commercial product of Rohm & Haas Co. designated as Plexiglas V(811). It is totally amorphous with $\bar{M}_n = 52,900$ g/mol and $\bar{M}_w = 130,000$ g/mol. Its glass transition temperature, T_g , measured by differential scanning calorimetry (DSC) is 106°C. The BCPC used here was kindly supplied by Dr. R. P. Kambour of the General Electric Co. It is also totally amorphous with a T_g of 164°C.

Films of the two homopolymers and their blends were prepared by solution casting. PMMA and BCPC in the desired ratio were dissolved in tetrahydrofuran (THF) at about 5% by weight total polymer and then cast onto a glass plate or an aluminum pan. The solvent was allowed to evaporate slowly at room temperature, and the formed films were dried in a vacuum oven at temperatures 20 to 30°C higher than their T_g 's. After drying, the films were quenched to ambient conditions. To investigate the solvent effect on blend-phase behavior, another solvent, chloroform, was also used to prepare the 50/50 blend whose state of mixing will be compared with the THF solution cast sample.

T_g 's for PMMA/BCPC blends were measured using a Perkin-Elmer DSC-2 differential scanning calorimeter equipped with a thermal analysis data station. The heating rate was 20°C/min and the onset of the change in heat capacity was defined as the T_g . The cloud points of the blends were measured using a hot plate on which the film was covered with a glass slide and heated until it became cloudy. To reduce thermal decomposition, the films were heated fast to temperatures about 30°C below the cloud point and then

heated slowly at 2°C/min to the cloud point and beyond. The temperature at which the clear film first started to become cloudy was taken as the cloud point.

Densities of the films were measured at 30°C by a density gradient column using aqueous solutions of calcium nitrate. These solution columns with density gradients less than 0.1 g/cm³ in each were prepared for samples of different density ranges.

The gas permeability coefficients for He, H₂, O₂, N₂, Ar, CH₄, and CO₂ at 35°C were measured by a high pressure permeation cell whose design and operation have been described elsewhere.^{27,28} Because gas permeabilities in glassy polymers are usually a function of pressure, the permeabilities were measured at near constant pressure conditions to facilitate development of a meaningful relationship with blend composition. For most cases the upstream side pressures were kept at 1 to 2 atm while the downstream side pressure was effectively zero. For N₂ and CH₄ with PMMA, the permeabilities were so low that higher upstream pressures up to 3–5 atm had to be used to enhance the accuracy of measurement.

RESULTS AND DISCUSSION

Phase Behavior

PMMA/BCPC blend films cast from THF solution were transparent which suggests they are miscible. DSC thermograms show that each blend has a single T_g intermediate between that of PMMA and BCPC (see Fig. 1). The T_g 's measured by DSC are plotted versus blend composition in Figure 2. For the 90% BCPC blend, the cast film shows a T_g somewhat below that of the arbitrarily drawn smooth curve for unknown reasons. However, this blend

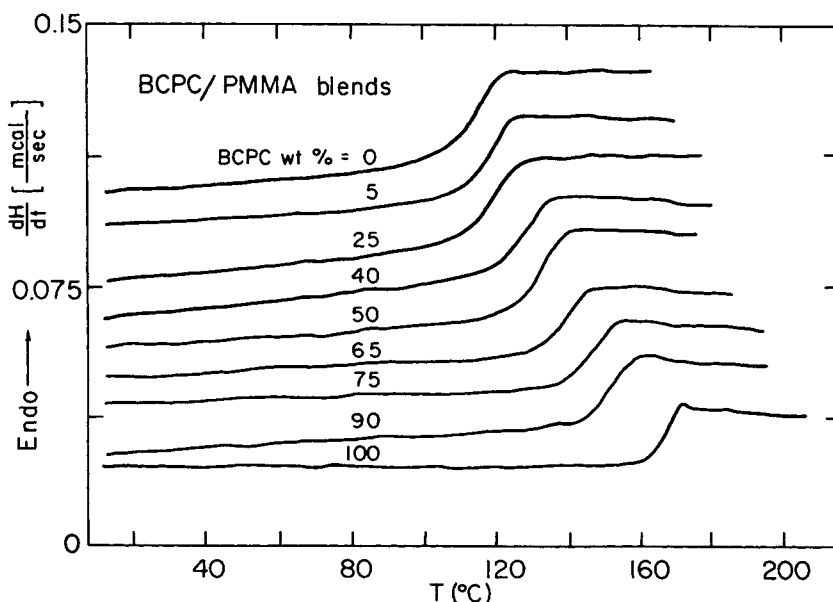


Fig. 1. Second heat DSC thermograms for PMMA/BCPC blends cast from THF solutions.

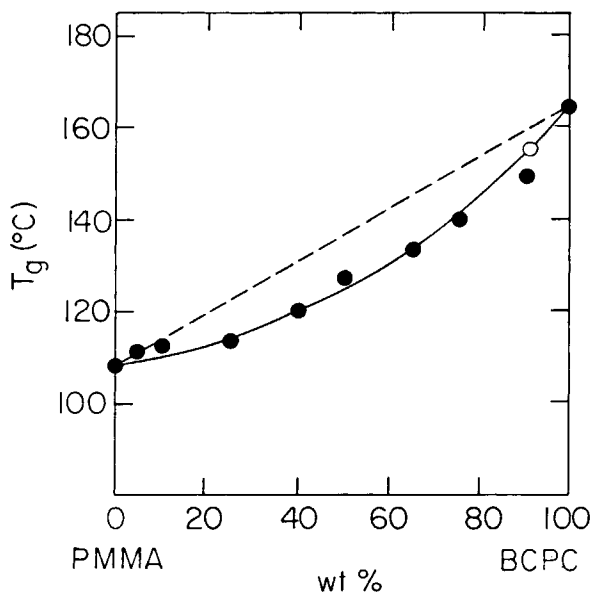


Fig. 2. Glass transition temperatures by DSC for PMMA/BCPC blends cast from THF solutions (solid points) and precipitated from methanol (open point).

prepared by precipitation using methanol as the nonsolvent gives a T_g on the curve.

It should be noted that phase behavior can be affected by the solvent choice when solution casting is used to prepare the blend. Blends which are miscible can phase separate during the course of solvent evaporation if there exists an immiscible region in the ternary phase diagram, that is, the solvent effect.²⁹⁻³¹ For instance, the 50% BCPC film cast from chloroform solution was trans-

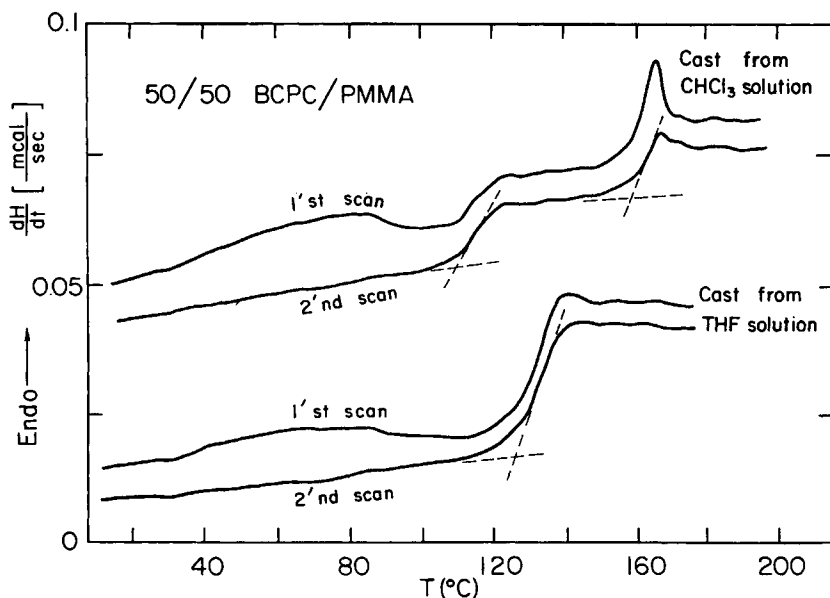


Fig. 3. Comparison of DSC thermograms for 50% blend cast from CHCl_3 and THF solutions.

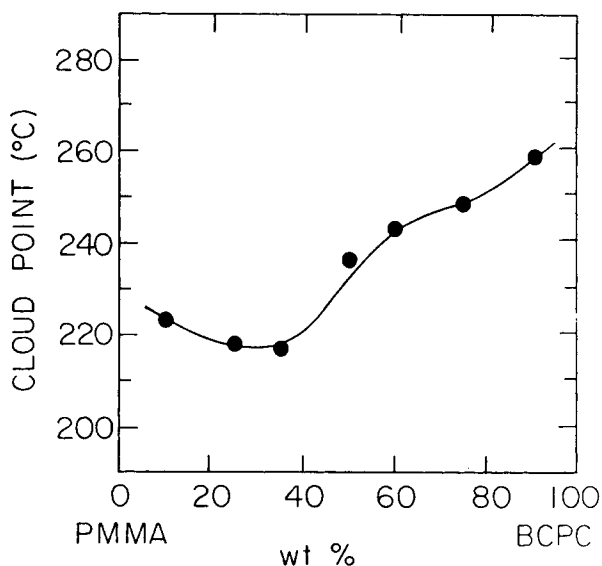


Fig. 4. Cloud points for PMMA/BCPC blends.

lucent, suggesting two phases exist in the blend. Figure 3 compares DSC thermograms of this blend cast from THF solution to that cast from chloroform solution. While the film cast from THF showed a single T_g , the film cast from chloroform showed two. The humps at 40 to 90°C in the first scans are due to relaxation of the pendent ester group in PMMA.^{32,33} The overshoot at the transition of BCPC for the chloroform cast film in the first scan is due to the sub- T_g annealing effect.³⁴⁻³⁶

It is well-known that phase separation may occur when a miscible blend is heated (i.e., lower critical solution (LCST) behavior).³⁷⁻³⁹ This phenomenon can be conclusive evidence that the blend is miscible. PMMA/BCPC blends exhibit phase separation on heating as shown in Figure 4.

SPECIFIC VOLUME

Previous studies for miscible polymer blends have shown that the specific volume of the blend, V , is often smaller than that calculated from linear additivity, V_{ideal} ,

$$V_{\text{ideal}} = V_1W_1 + V_2W_2 \quad (2)$$

where W is the weight fraction and subscripts 1 and 2 denote the two components. This phenomenon can be the result of denser packing of the polymer chains owing to the favorable interaction between the component polymers which promotes miscibility. The magnitude of the contraction expressed as the residual volume, V_{res} ,

$$V_{\text{res}} = V - V_{\text{ideal}} \quad (3)$$

is qualitatively an indicator of the extent of this interaction. Figure 5 shows the densities, specific volumes, and residual volumes of PMMA/BCPC blends. The specific volumes closely follow the simple additive rule. The residual

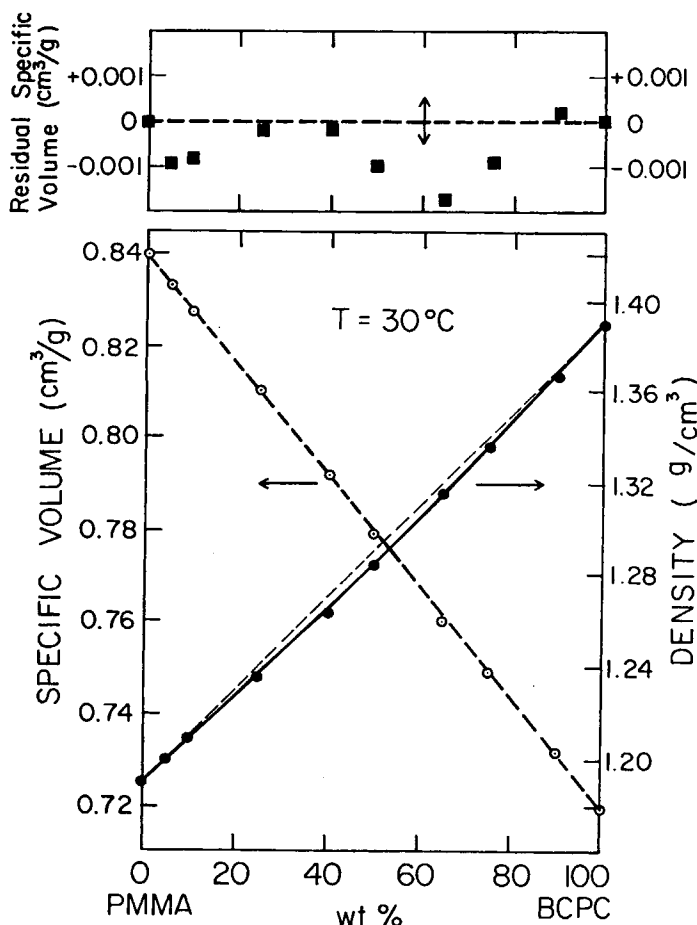


Fig. 5. Densities and specific volumes of PMMA/BCPC blends at 30°C. Upper part shows residual specific volumes on expanded scale, the arrow bar indicates the error range.

volumes are as small as the experimental errors, $\pm 0.0005 \text{ g/cm}^3$, indicating the interaction between PMMA and BCPC must be relatively weak.

GAS PERMEATION

Figures 6 to 11 show permeability coefficients for all gases used here plotted semilogarithmically versus volume fraction of BCPC in the blend. As seen, gas permeabilities for the blends are lower than those calculated from Eq. (1) represented by the dashed lines in Figures 6-11. Similar results have been found before for several other miscible blend systems, for example, polystyrene with poly(phenylene oxide)¹⁴ and polycarbonate with a copolyester.¹⁸ On the other hand, opposite cases where gas permeabilities follow the semi-logarithmic linearity⁴ or even a positive deviation⁴⁰ have also been observed.

To explain the various ways in which gas permeability can depend on blend composition, the free volume theory and the activated state theory have been used. In the free volume theory,^{13,41} the gas permeability of the blend is related to that of the two component polymers by

$$\ln(P/A) = [\phi_1/\ln(P_1/A) + \phi_2/\ln(P_2/A)]^{-1} \quad (4)$$

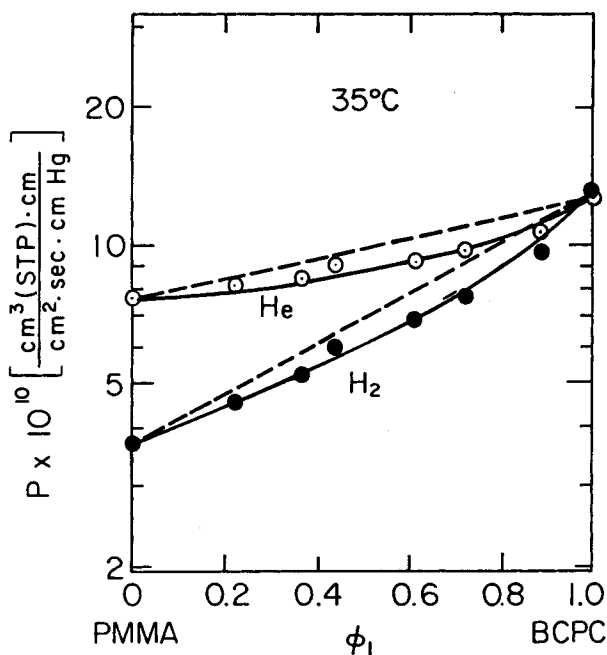


Fig. 6. Semilogarithmic plots of He and H₂ permeabilities vs. volume fraction of BCPC in blends.

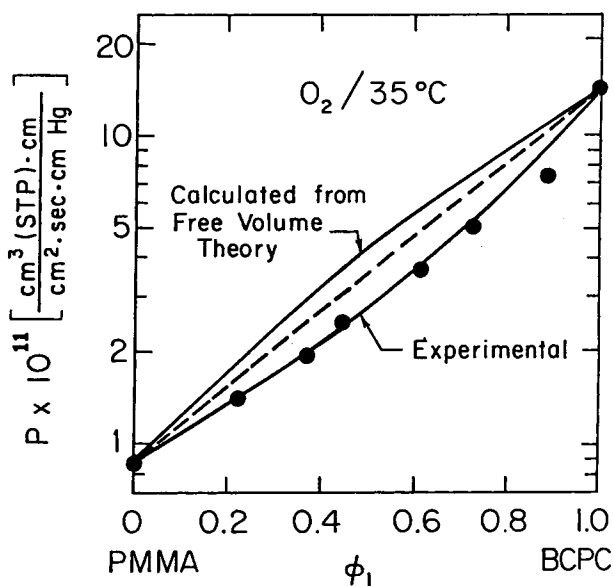


Fig. 7. Semilogarithmic plot of O₂ permeabilities vs. volume fraction of BCPC in blends.

where A is a characteristic constant for a gas. According to this equation which assumes additivity of free volume, the gas permeability of the blend will be higher than that calculated from Eq. (1) so long as P_1 and P_2 are substantially different. When P_1 and P_2 are similar in magnitude, then Eq. (4) reduces to Eq. (1) (see Appendix). If there exists a significant volume contrac-

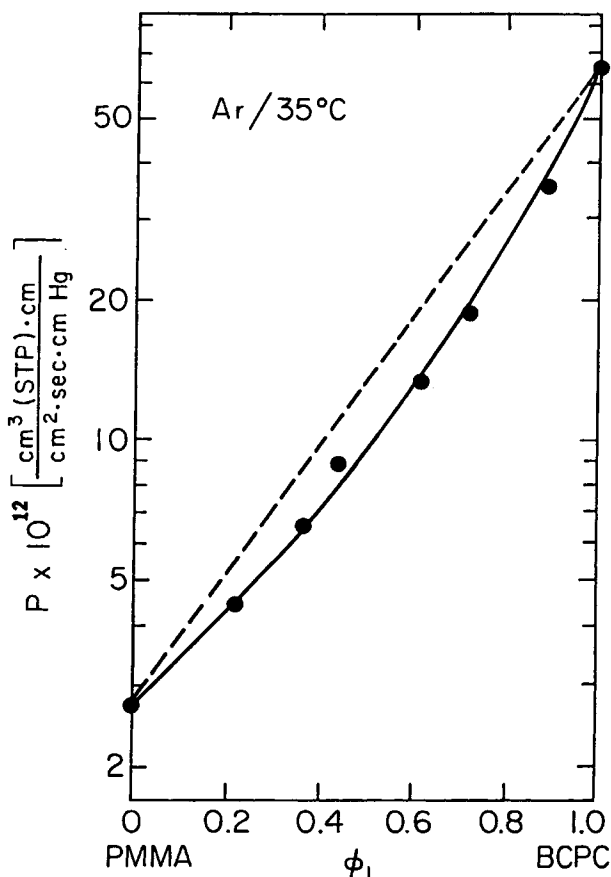


Fig. 8. Semilogarithmic plot of Ar permeabilities vs. volume fraction of BCPC in blends.

tion for the blend, then the permeability will be lower than that predicted by Eq. (4).¹³ For PMMA/BCPC blends, the correction for this effect is negligible since the volume contraction is small (see Fig. 5). The permeabilities for O₂, CH₄, and CO₂ calculated from Eq. (4) are also shown in Figures 7, 10, and 11 using values for A of 7.9×10^{-7} ,¹³ 2.2×10^{-6} , and 6.6×10^{-6} [cm³ (STP) · cm/cm² · cm Hg · s],⁴² respectively. Obviously, gas permeabilities predicted from the free volume theory are significantly higher than the measured ones.

In the activated state theory, the diffusion of a small molecule in a blend is described by

$$\ln D = \phi_1 \ln D_1 + \phi_2 \ln D_2 + (\alpha RT - 1) \Delta E_{12} / RT \quad (5)$$

where D is the diffusion coefficient, α is a constant which gives $(\alpha RT - 1)$ a negative value of approximately -0.5 , R is the gas constant, T is the temperature, and ΔE_{12} is the deviation term for the activation energy, E_D , defined as

$$E_D = \phi_1 E_{D1} + \phi_2 E_{D2} + \Delta E_{12} \quad (6)$$

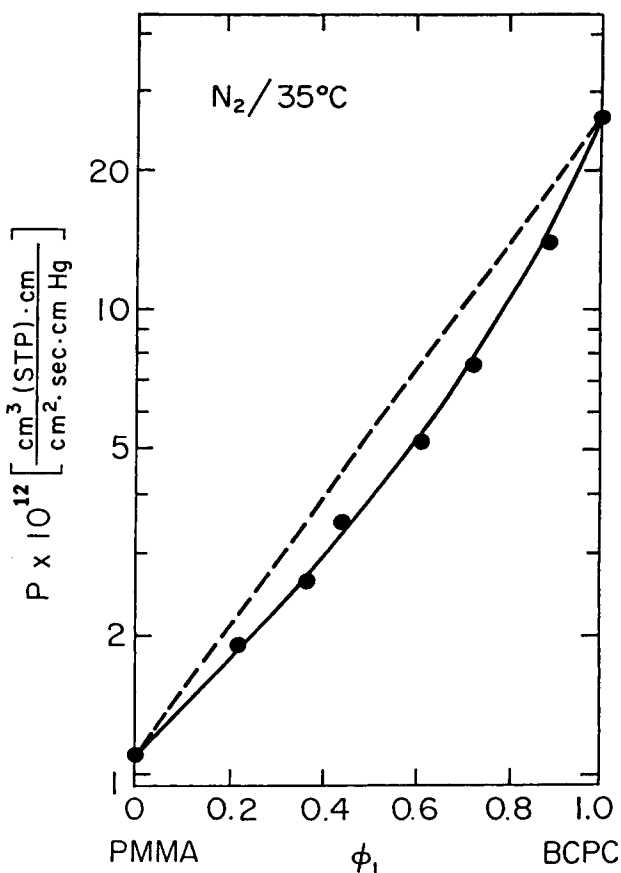


Fig. 9. Semilogarithmic plot of N_2 permeabilities vs. volume fraction of BCPC in blends.

From ternary solution theory,^{1,18,43} it has been shown that the solubility coefficient, S , for the blend can be related to that of the components by

$$\ln S = \phi_1 \ln S_1 + \phi_2 \ln S_2 + (BV_3/RT)\phi_1\phi_2 \quad (7)$$

where B is the binary interaction parameter for the blend and V_3 is the molar volume of the penetrant. The permeability coefficient is the product of the diffusion coefficient and the solubility coefficient, i.e.,

$$P = DS \quad (8)$$

Combining Eqs. (5) and (7) yields

$$\ln P = \phi_1 \ln P_1 + \phi_2 \ln P_2 + (\alpha RT - 1)\Delta E_{12}/RT + (BV_3/RT)\phi_1\phi_2 \quad (9)$$

Compared to Eq. (1), Eq. (9) has two excess terms. As we will show later, these two terms are all negative for PMMA/BCPC blends which results in the negative deviations observed in Figures 6-11.

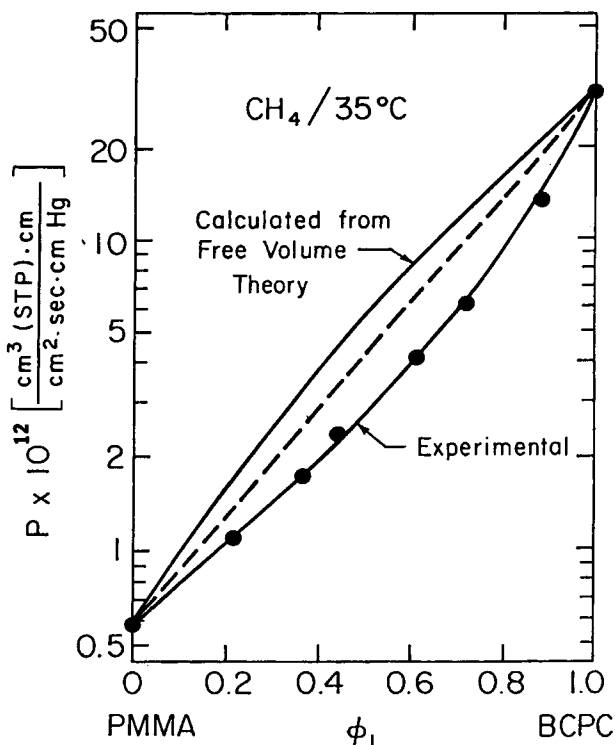


Fig. 10. Semilogarithmic plot of CH₄ permeabilities vs. volume fraction of BCPC in blends.

Since gas diffusion and solubility coefficients in glassy polymers like PMMA and BCPC are functions of pressure, true sorption and diffusion parameters can only be obtained from sorption and permeation experiments over a wide pressure range. For an approximation, however, the gas diffusion coefficient can be represented by an apparent value, D_a , measured from the time-lag method, that is,

$$D_a = \ell^2 / 6\theta \quad (10)$$

where ℓ is the film thickness and θ is the diffusional time lag. Figures 12–16 show the semilogarithmic plots of apparent diffusion coefficients of various gases versus volume fraction of BCPC in the blend. As shown, the apparent diffusion coefficients are lower than predicted from semilogarithmic additivity. Thus, according to Eq. (5), the excess term must be negative, or, ΔE_{12} is positive since $(\alpha RT - 1)$ is negative. This means that the activation energy for gas diffusion in the blend is higher than the sum of additive contributions [see Eq. (6)]. Such a result suggests that the activation process for a gas to jump from one site to another requires more energy for the blend than expected from contributions of the pure components presumably because of the interactions between the component polymer molecules in the blend.

To examine how gas solubilities in PMMA/BCPC blends are related to blend composition, an apparent gas solubility coefficient defined as

$$P = D_a S_a \quad (11)$$

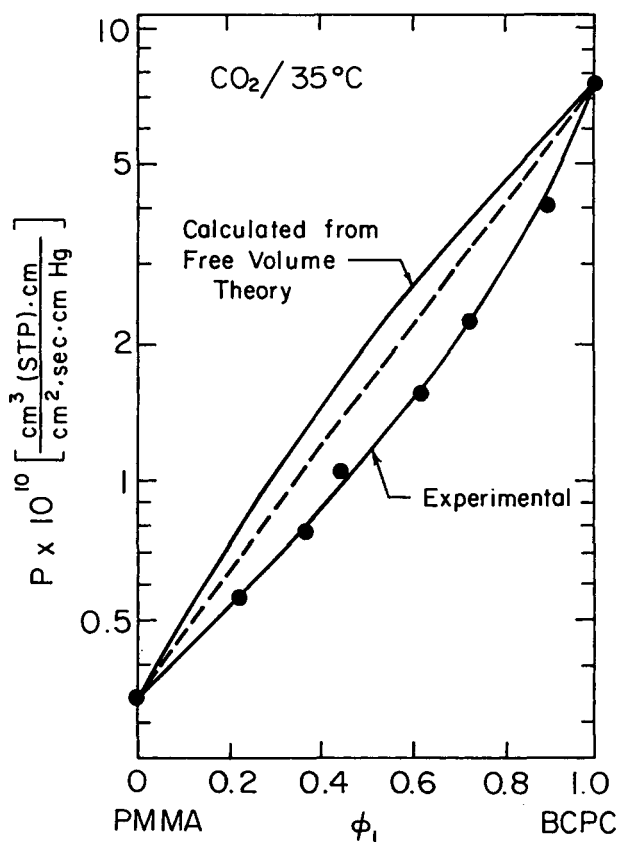


Fig. 11. Semilogarithmic plot of CO₂ permeabilities vs. volume fraction of BCPC in blends.

is adopted here. Using the permeability and apparent diffusivity reported above, the apparent solubility coefficients for various gases in the blends are calculated and presented in Figure 17. Again, negative deviations are observed. This result is predicted since for miscible blends the binary interaction parameter, B , is negative which leads to a negative excess term in Eq. (7). No efforts were made to estimate B value from this result because the apparent solubility observed in Figure 17 does not represent the Henry's law solubility defined in Eq. (7).

IDEAL GAS SEPARATION FACTOR

Since gas separations by membranes have been of intensive interest in recent years, it would be interesting to examine the potential of applying miscible blends for gas separation. In practice, the true separation factor for a gas pair A and B is measured from the ratio of their permeation rates using gas mixtures as the penetrant. For an estimate, however, this permselectivity characteristic can be obtained by examining the ratio of gas permeabilities of the two pure gases, namely, the ideal gas separation factor for gas A relative

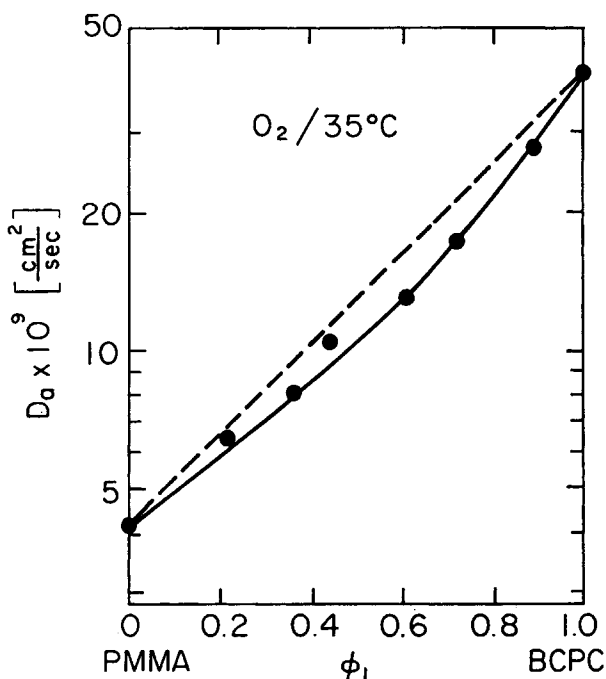


Fig. 12. Semilogarithmic plot of O_2 apparent diffusion coefficients vs. volume fraction of BCPC in blends.

to gas B defined as

$$\alpha_B^A = P_A/P_B \quad (12)$$

It should be noted that the ideal gas separation factor may be different from the actual one measured from mixed gas experiments for two reasons. First, the two gases when mixed may compete for sorption sites in glassy polymers leading to different sorption and transport behavior from the pure gases.^{44, 45} Second, when one of the gases has much higher solubility than the other, its plasticizing effect could change the diffusion coefficient of the other, which cannot easily be estimated from pure gas experiments.

Three gas pairs of some practical interest, namely, He/CH_4 , CO_2/CH_4 , and O_2/N_2 , are considered below for their permselectivity characteristics. Figures 18 and 19 show the ideal separation factors plotted versus blend composition. Contrary to the negative deviation behavior for permeability, the ideal separation factors are higher than that of the semilogarithmic additivity rule. Note that if gas permeation behavior in the blend follows Eq. (1), in other words, the semilogarithmic additivity rule, then a similar mixing rule can be derived for gas separation, namely,

$$\ln \alpha_B^A = \phi_1 \ln(\alpha_B^A)_1 + \phi_2 \ln(\alpha_B^A)_2 \quad (13)$$

as represented by the dashed lines in Figures 18 and 19.

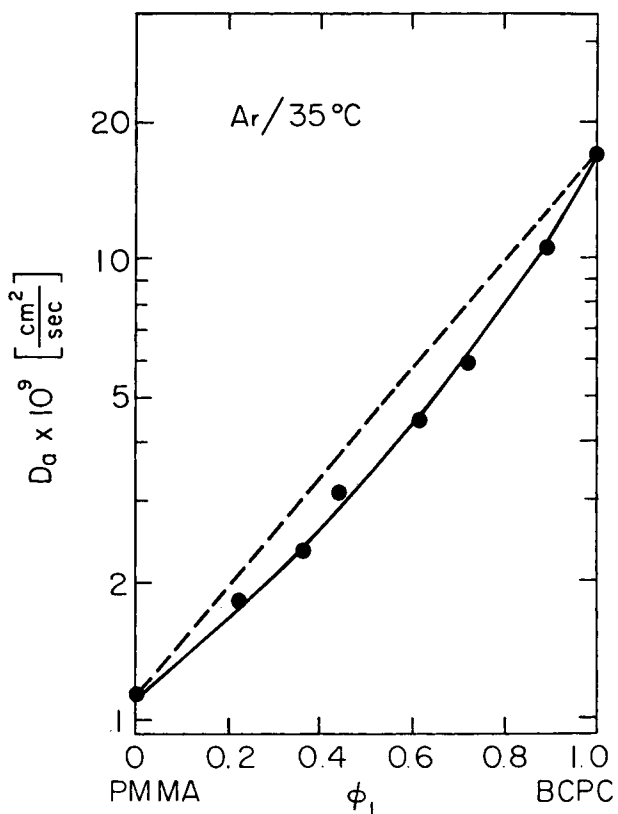


Fig. 13. Semilogarithmic plot of Ar apparent diffusion coefficients vs. volume fraction of BCPC in blends.

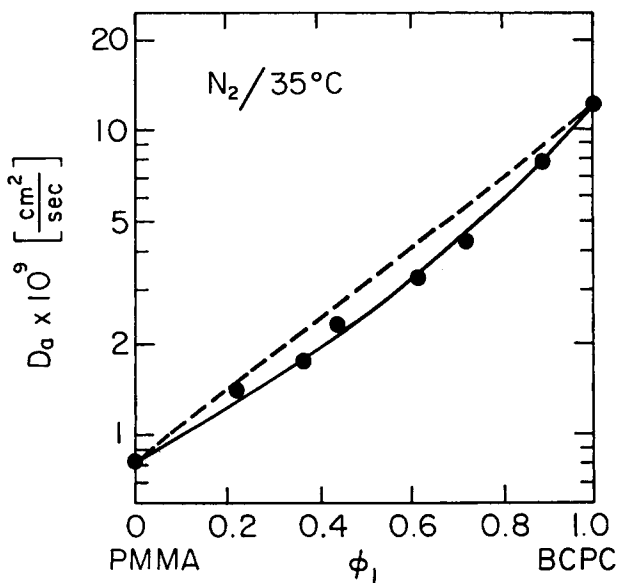


Fig. 14. Semilogarithmic plot of N_2 apparent diffusion coefficients vs. volume fraction of BCPC in blends.

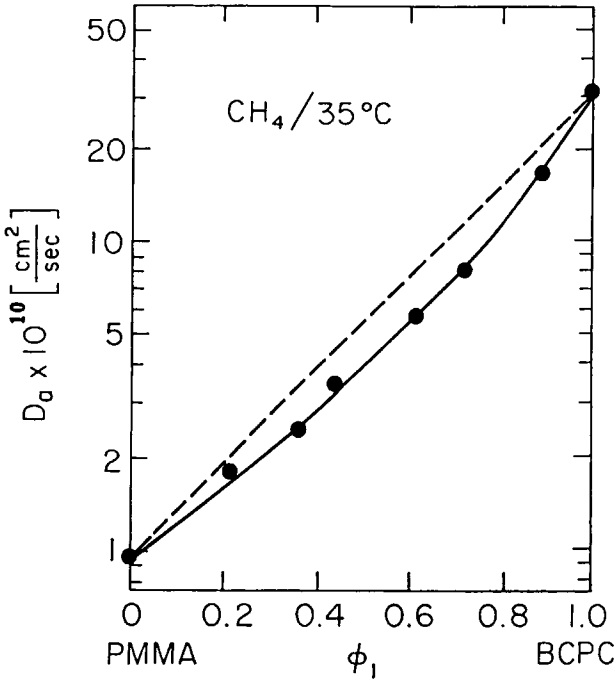


Fig. 15. Semilogarithmic plot of CH_4 apparent diffusion coefficients vs. volume fraction of BCPC in blends.

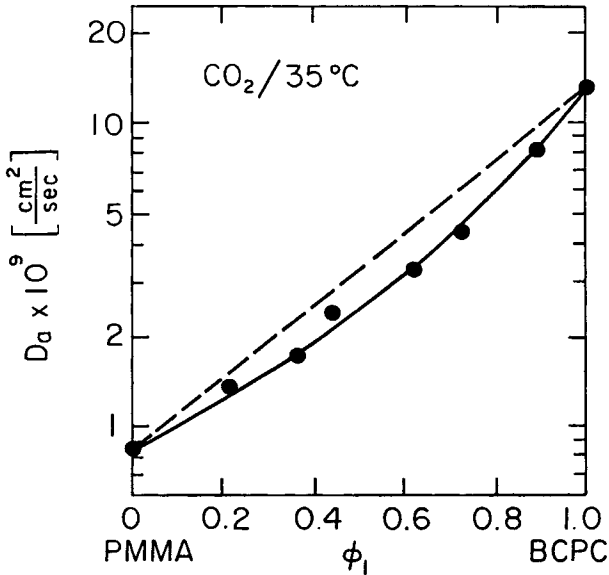


Fig. 16. Semilogarithmic plot of CO_2 apparent diffusion coefficients vs. volume fraction of BCPC in blends.

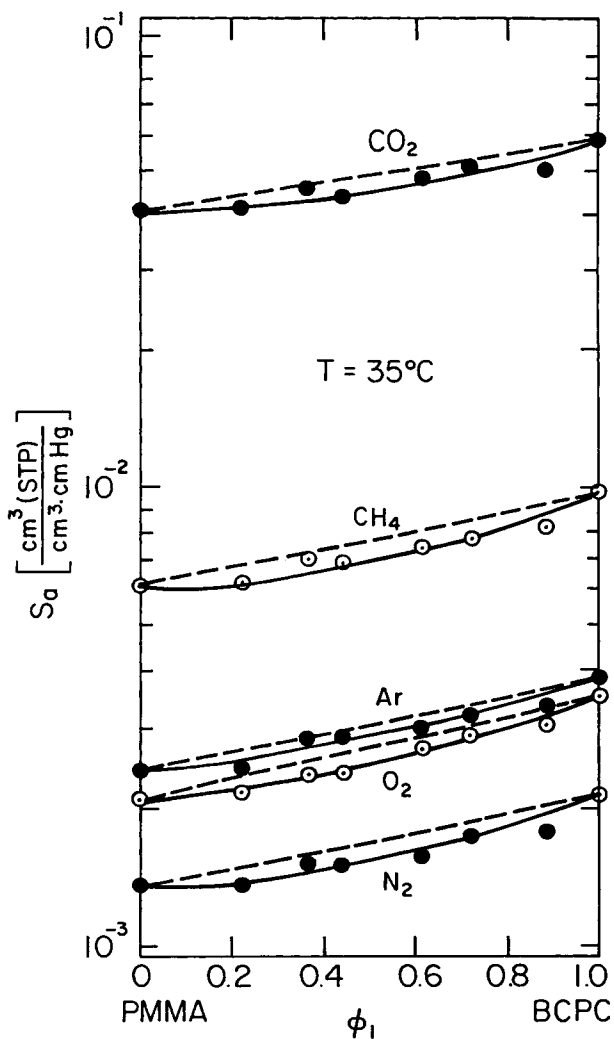


Fig. 17. Semilogarithmic plot of apparent solubility coefficients vs. volume fraction of BCPC in blends.

Figures 6–11 not only show that the gas permeability is lower than that from the linear additivity rule but the extent of deviation increases with gas molecular size, that is, the smallest for He and the largest for CH_4 . This causes the positive deviation for the ideal separation factor. The He/CH_4 pair exhibits deviations larger than CO_2/CH_4 and O_2/N_2 pairs do because He and CH_4 differ the most in molecular size. Similar results have been observed for several other miscible blend systems.^{14–18} In cases where the two component polymers have similar separation factors, the separation factors of the blends can be even higher than that of the two components.^{14,15} This suggests that better gas permselectivity could be achieved through blending of two miscible polymers.

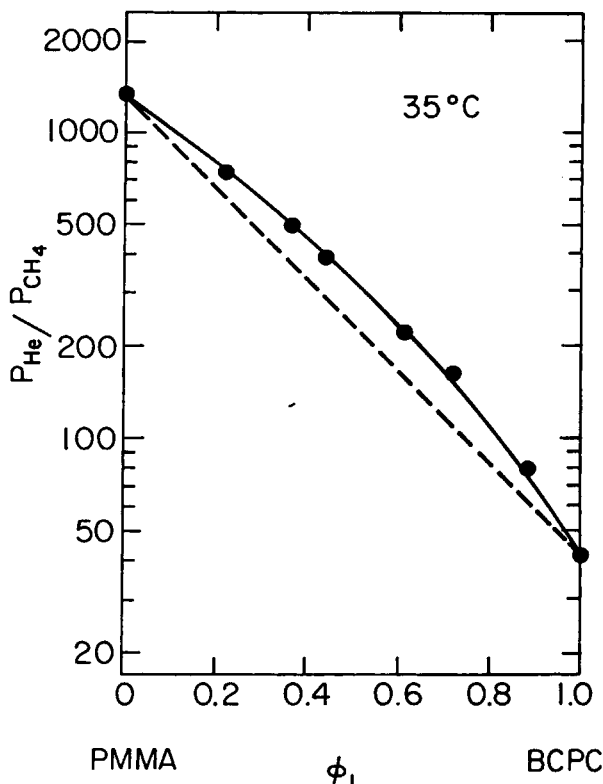


Fig. 18. Semilogarithmic plot of ideal separation factors for He/CH₄ pair vs. volume fraction of BCPC in blends.

CONCLUSIONS

This study has shown that poly(methyl methacrylate) and bisphenol chloral polycarbonate are miscible over the entire blend composition range. DSC thermograms reveal a single composition-dependent glass transition for each blend. Lower critical solution temperature (LCST) behavior has also been observed, as when transparent blends turn to cloudy when heated to high temperatures. Density measurements suggest that the interaction between PMMA and BCPC is evidently weak because the specific volumes of the blends closely follow the additivity rule.

The permeability coefficients for various gases in the blends are lower than that calculated from the semilogarithmic additivity rule. Moreover, the magnitude of this deviation increases with molecular size, which results in ideal separation factors higher than expected from the semilogarithmic linearity for He/CH₄, CO₂/CH₄, and O₂/N₂ gas pairs. These permeation results can be explained by the activated state theory for gas diffusion and the ternary solution theory for gas solution in miscible blends. Both the apparent diffusion and solubility coefficients for the blends also show negative deviation from the semilogarithmic additivity rule.

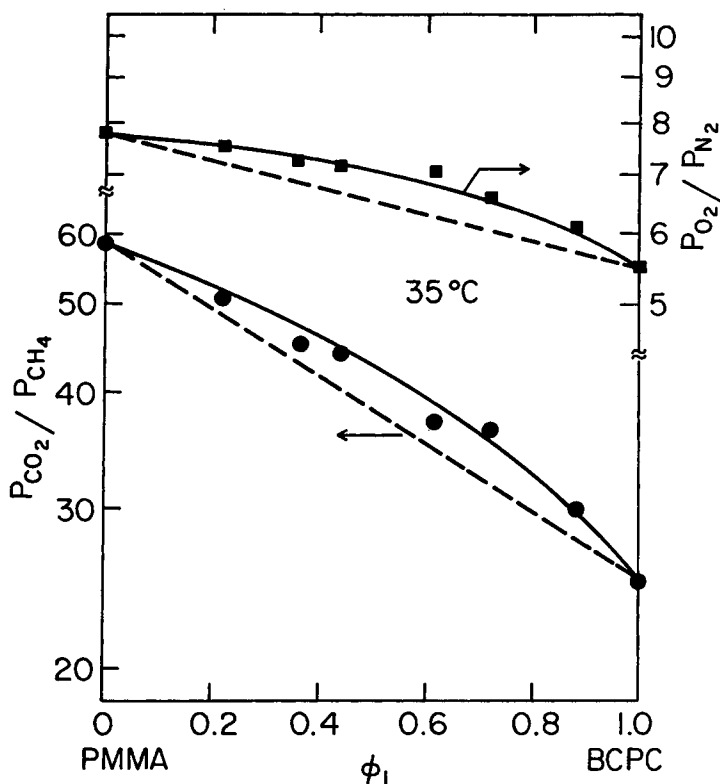


Fig. 19. Semilogarithmic plot of ideal separation factors for CO_2/CH_4 and O_2/N_2 pairs vs. volume fraction of BCPC in blends.

This research was supported by the University of Texas Separations Research Program, the U. S. Army Research Office, and the donors of the Petroleum Research Fund, administered by the American Chemical Society.

APPENDIX

A simple free volume treatment assuming additivity of free volume, or no volume change on mixing, gives Eq. (4) as the mixing rule for permeability in multicomponent polymer systems.¹³ In general, Eq. (4) predicts permeability values which lie above the linear relation on semilogarithmic coordinates given by Eq. (1), but for some circumstances Eq. (4) gives essentially equivalent results as Eq. (1). The purpose here is to examine more closely the differences between Eqs. (1) and (4) and to see when they give comparable results.

As suggested by the inset in Figure 20, let P_o be the prediction of Eq. (1) and P be the prediction of Eq. (4) for a given composition. By algebraic rearrangements of these two equations, we can show that

$$\ln(P/P_o) = - \frac{[\ln(P_2/P_1)]^2}{2[2\ln(P_1/A) + \ln(P_2/P_1)]} \quad (14)$$

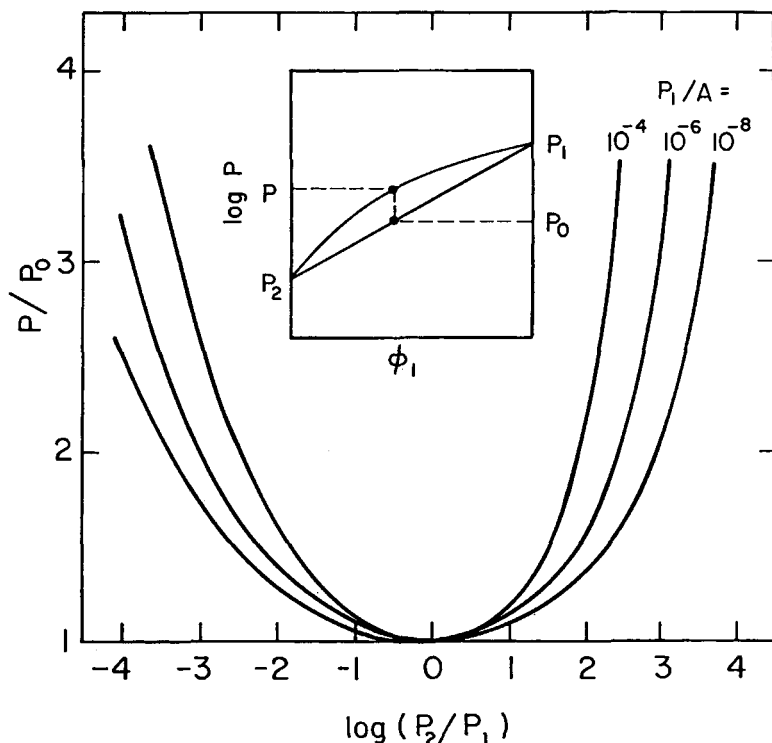


Fig. 20. Deviation of the permeability predicted by additive free volume model, P , from the linear semilogarithmic relation given by Eq. (1), i.e., P_0 .

This result is plotted in Figure 20 with the factor P/P_0 given as a function of the ratio of the permeabilities of the two pure polymers for different absolute levels of permeability relative to the constant A . As can be seen, the difference between the predictions of Eqs. (1) and (4) vanish as P_2 approaches P_1 . In fact, the difference is only of the order of 10% when P_2 and P_1 differ by a factor of 10.

References

1. H. B. Hopfenberg and D. R. Paul, *Polymer Blends*, Vol. I, D. R. Paul and S. Newman, Eds., Academic, New York, 1978, Chap. 10.
2. B. G. Ranby, *J. Polym. Sci. Symp.*, **51**, 89 (1975).
3. Y. J. Shur and B. Ranby, *J. Appl. Polym. Sci.*, **19**, 89 (1975).
4. J. S. Chiou, J. W. Barlow, and D. R. Paul, *J. Appl. Polym. Sci.*, **30**, 1173 (1985).
5. L. M. Robeson, A. Noshay, M. Matzner, and C. N. Merriam, *Die Anrew. Makromol. Chem.*, **29 / 30**, 47 (1973).
6. A. E. Barnabeo, W. S. Creasy, and L. M. Robeson, *J. Polym. Sci. Polym. Chem. Ed.*, **13**, 1979 (1975).
7. Y. J. Shur and B. Ranby, *J. Appl. Polym. Sci.*, **19**, 1337 (1975).
8. Y. J. Shur and B. Ranby, *J. Appl. Polym. Sci.*, **19**, 2143 (1975).
9. Y. J. Shur and B. Ranby, *J. Appl. Polym. Sci.*, **20**, 3105 (1976).
10. Y. J. Shur and B. Ranby, *J. Appl. Polym. Sci.*, **20**, 3121 (1976).
11. Y. J. Shur and B. Ranby, *Macromol. Sci.-Phys.*, **B14**, 565 (1977).
12. E. L. Nikishin, A. E. Chalykh, A. Avgonov, V. N. Kuleznev, L. V. Morozova, and A. N. Neverov, *Colloid. J.*, **40**, 660 (1979).

13. D. R. Paul, *J. Membrane Sci.*, **18**, 75 (1984).
14. Y. Maeda and D. R. Paul, *Polymer*, **26**, 2055 (1985).
15. A. Murugananadam and D. R. Paul, to be published.
16. J. S. Chiou and D. R. Paul, *J. Appl. Polym. Sci.*, in press.
17. J. S. Chiou and D. R. Paul, *J. Appl. Polym. Sci.*, in press.
18. P. Masi, D. R. Paul, and J. W. Barlow, *J. Polym. Sci. Polym. Phys. Ed.*, **20**, 15 (1982).
19. W. E. Preston, J. W. Barlow, and D. R. Paul, *J. Appl. Polym. Sci.*, **29**, 845 (1984).
20. A. Factor and C. M. Orlando, *J. Polym. Sci. Polym. Chem. Ed.*, **18**, 579 (1980).
21. R. J. Peterson, R. D. Corneliussen, and L. T. Rozelle, *Polym. Prepr. Amer. Chem. Soc., Div. Polym. Chem.*, **10**, 385 (1969).
22. Z. G. Gardlund, *Polym. Prepr.*, **23**, 258 (1982).
23. I. N. Razinskaya, B. S. Galle, L. I. Ott, L. P. Bubnova, L. I. Batuyeva, N. I. Pupukina, L. V. Adamova, and B. P. Shtarkman, *Polym. Sci. USSR*, **27**, 204 (1985).
24. Z. G. Gardlund, *ACS Symp. Series*, **206**, 129 (1984).
25. K. K. Koo, T. Inoue, and K. Miyasaka, *Polym. Eng. Sci.*, **25**, 741 (1985).
26. J. S. Chiou, J. W. Barlow, and D. R. Paul, *J. Polym. Sci. Polym. Phys. Ed.*, in press.
27. W. J. Koros, D. R. Paul, and A. A. Rocha, *J. Polym. Sci. Polym. Phys. Ed.*, **14**, 687 (1976).
28. W. J. Koros and D. R. Paul, *J. Polym. Sci. Polym. Phys. Ed.*, **14**, 1903 (1976).
29. L. Zeman and D. Patterson, *Macromolecules*, **5**, 513, (1972).
30. A. Robard and D. Patterson, *Macromolecules*, **10**, 706 and 1021 (1977).
31. D. Patterson, *Polym. Eng. Sci.*, **22**, 64 (1982).
32. N. G. McCrum, B. E. Read, and G. Williams, *Anelastic and Dielectric Effects in Polymeric Solids*, John Wiley & Sons, New York, 1967, Chap. 8.
33. F. Lednický and J. Janacek, *J. Macromol. Sci. Phys.*, **B5**, 335 (1971).
34. I. M. Hodge and A. R. Berens, *Macromolecules*, **14**, 1598 (1981).
35. I. M. Hodge and A. R. Berens, *Macromolecules*, **15**, 756 (1982).
36. I. M. Hodge and G. S. Huvard, *Macromolecules*, **16**, 371 (1983).
37. T. Nishi and T. K. Kwei, *Polymer*, **16**, 285 (1975).
38. P. Alexandrovich, F. E. Karasz, and W. J. MacKnight, *Polymer*, **18**, 1022 (1977).
39. D. R. Paul and J. W. Barlow, *J. Macromol. Sci., Rev. Macromol.*, **C18**, 109 (1980).
40. J. S. Chiou and D. R. Paul, *J. Appl. Polym. Sci.*, in press.
41. W. M. Lee, *Polym. Eng. Sci.*, **20**, 65 (1980).
42. Y. Maeda, dissertation, Univ. of Texas at Austin, 1986.
43. G. Morel and D. R. Paul, *J. Membrane Sci.*, **10**, 273 (1982).
44. W. J. Koros, R. T. Chern, V. Stannett, and H. B. Hopfenberg, *J. Polym. Sci. Polym. Phys. Ed.*, **19**, 1513 (1981).
45. R. T. Chern, W. J. Koros, E. S. Sanders, S. H. Chen, and H. B. Hopfenberg, *ACS Symp.*, **223**, 47 (1983).

Received September 9, 1986

Accepted November 10, 1986